Title:

# Moisture migration on the shear zone controls landslide failure models

Author: Fanyu Zhang[a*], Gonghui Wang[b], Jianbing Peng[c]

Affiliation:

(a): MOE Key Laboratory of Mechanics on Disaster and Environment in Western China, Department of Geological Engineering, Lanzhou University, Lanzhou 730000, Gansu, China

(b): Research Center on Landslides, Disaster Prevention Research Institute, Kyoto University, Gokasho, Uji, Kyoto, 611-0011, Japan

(c) Department of Geological Engineering, Chang'an University, Xian, Shaanxi Province 710054, China

Corresponding author: Fanyu Zhang

Email: Zhangfy@lzu.edu.cn

Title: **Moisture migration on the shear zone controls landslide failure models**

Author: Fanyu Zhang, Gonghui Wang, Jianbing Peng

**Abstract:** The shear behavior of loess is of paramount importance to understanding of mechanisms triggering landslides. In this research, using a ring shear apparatus, a series of ring-shear tests was performed on the Lanzhou loess to examine the residual shear behavior of the loess with different water contents. The results show that the increase of water content results in the reduction of void ratio of the samples, when the water content continuously increase to a special threshold, the void ratio of the samples increase lightly then reach a stable state. Correspondingly, the cohesion increase and the friction angle decrease with increasing water content until the water content threshold, and thereafter the cohesion decreased quickly to zero and the friction angle stabilized at a residual value. Futhermore, the localization of shear deformation result in difference between shear zone and soli layers below and above the shear zone in void ratio, causing the two different types of water migration on shear zone. Before the water content threshold, the water is sucked towards shear zone from soil layers above and below the shear zone, and then the water is expelled shear zone into soil layers above and below the shear zone. The water migration can influence shear strength of soil which depends on the type of water migration on shear zone. These results reveal that the volumetric change of soil not only has great influence on shear behavior during wetting but also is related to the water migration during shearing.

**Keywords: Loess landslide, shear zone, volumetric response, water migration, residual shear strength, ring shear tests**

## 1 Introduction

Landslides occurred in loess setting cause serious casualties and much destruction almost every year. Loess landslides are often triggered by rainfall and irrigation (Gibbs and Holland, 1960; Lutenegger and Hallberg, 1988; Derbyshire et al., 1991; Derbyshire et al., 1994; Dijkstra et al., 1994; Derbyshire, 2001; Ueno et al., 2005), but sometimes earthquake is also an important trigger to them (Lutenegger, 1981; Ishihara et al., 1990; Zhang and Wang, 2007). In these conditions, the initiation and movement of loess landslides were generally implicated in reduction of shear strength of soil accompanied by gradual or rapid increase of water content.

There has been considerable research into examining the effect of water content on shear strength of loess, and much of this effort has recognized that the impacts of water content are of paramount importance to understanding the mechanisms of loess landslides (Gibbs and Holland, 1960; Lutenegger, 1981; Ishihara et al., 1990; Derbyshire et al., 1994; Dijkstra et al., 1994; Zhang and Wang, 2007; Zhang et al., 2009). Most of the previous studies were performed on undisturbed loess samples in triaxial tests, mainly focusing on the natural and saturated samples (Gibbs and Holland, 1960; Audric and Bouquier, 1976; RenéJacques, 1988; Tan, 1988; Abduljauwad and Al-Gassous, 1991; Phien-wej et al., 1992; Zhang et al., 2009). Additionally, there have been few attempts to examine shear strength behavior of remolded loess samples in ring shear tests (Derbyshire et al., 1994; Dijkstra et al., 1994; Zhang and Wang, 2007). Derbyshire et al. (1994) and Dijkstra et al. (1994) conducted a series of tests at different water contents on remolded loess samples taken from Chinese Lanzhou region, using a modified Bromhead ring shear apparatus. The results showed that the apparent cohesion increased and the internal friction angle decreased with increasing water content untill a certain threshold, after which the apparent cohesion decreased rapidly and the internal friction angle stabilized at a residual value theoretically. In practice, however, the leakage of water and fine particle during shearing caused an increase in the internal friction angle due to the deficiencies of the apparatus (Derbyshire et al., 1994). Derbyshire et al. (1994) also pointed out that the leakage also affected the cohesion of soil. Hence, we can find that change in water content during shearing has impact on strength behavior of the loess. Furthermore, field investigation to four loess landslides have shown that the water content on shear zone is higher than that of soil mass above and below the shear zone (Long et al., 2007). The authors hypothesized that the shear zones were related to pedological soil acting upon a relatively impermeable layer, causing higher water content on shear zone. To the phenomena existed, we need more detailed study to clarify the effect of water content change on strength behavior of a soil during wetting and shearing.

However, the strength behaviors of soil under different water contents dry to saturated conditions have been studied in less detail. Furthermore, there is no research concerned with water change within samples with various water contents during shearing and its relation with strength behavior of soil.

In this paper, we examine loess samples taken from a landslide, occurring on Jiuzhoutai area of Lanzhou City, China. The approach of our research is to investigate experimentally, using a ring shear apparatus, the strength behavior of the loess samples suffered large shear displacement at different normal stresses by varying water content. The main purpose of our research is to study the effect of water content on residual strength behavior of the loess. We focus on analyzing variation of residual shear strength parameters (cohesion and friction angle) of soil with different water contents, and pay special attention to the water content change at different layers within samples after shearing and its relation with the residual shear strength parameters. The results of our research showed that water migration on shear zone can afford a new understanding to mechanisms triggering loess landslides, especially in unsaturated settings.

## 2 Material and methods

### 2.1 Testing sample

We took loess samples from a landslide, occurring on Jouzhoutai area of Lanzhou city, Gansu Province, China (Fig. 1). Many landslides occurred without direct triggers such as rainfall or earthquake, and this landslide was a typical case. Despite the modest volume involved, this kind of landslide has caused many fatalities and much destruction, due to their high velocity along steep slope and the absence of incipient movement evidence.

The loess is an aeolian silt with a mean particle diameter of 0.018, coefficient of uniformity of 5.50 and coefficient of gradation of 1.05. The grain size distribution of the loess samples is presented in Fig. 2. The sample approximately is consisted of about 92% silt, 7% clay and 1% sand. Some basic physical properties of the samples are listed in Table 1. It has low plastic limit, low in-situ bulk density and greatly natural void ratio.

## 2.2 Sample preparation

The samples were prepared in terms of different initial water contents. Distilled water was first added to oven dried samples to reach the desired water contents and the samples were stirred evenly. Then, the samples were sealed by thin plastic film and stored for 24 hours in an air-conditioned room such that the sample has uniform distribution of moisture. After that, the prepared samples were placed in the shear box using moist tamping method (Finno et al., 1997).

This method has the advantage that high void ratio specimen can be easily achieved (Finno et al., 1997). The samples were placed in three layers, and then each layer was damped to obtain the designed densities.

## 2.3 Testing apparatus

The ring shear apparatus has been widely used in examining the residual shear strength of soils for the analysis of slope stability (Bishop et al., 1971; Bromhead, 1979; Sassa et al., 2004; Wang and Sassa, 2009; Wang et al., 2010). The ring shear apparatus employed in the present research is the fifth version (DPRI-5), which was developed by Disaster Prevention Research Institute (DPRI), Kyoto University (Sassa et al., 2004). The apparatus has a shear box with 120 mm inner diameter, 180 mm outer diameter, 115 mm height. The apparatus allows shear tests on soils under drained or completely undrainded condition. The apparatus has also a special structure that prevents soil or water leakage during long shear displacement.

The schematic of the ring-shear apparatus is shown in Fig 3. The overview of the apparatus is shown in Fig. 3a. The shear mode of a sample in the torque-controlled ring-shear apparatus was shown conceptually in Fig. 3b. The sample in the ring-shear box is laterally confined between pairs of doughnut-shaped upper and lower confining rings. During the test, the sample is loaded normally through an annular loading platen connected to a load piston. The lower half of the shear box rotates in both directions, driven by a servomotor through a transmission system, while the upper part is kept steady by means of two retaining torque arms. Fig. 3c illustrates enlarged diagram of half of the cross section the undrained ring-shear box and the pore-water pressure measurement system. The detailed information on ring shear tests can be found in relevant literatures (Wang and Sassa, 2002; Sassa et al., 2003).

### 2.4 Testing program and procedure

To measure the cohesion and friction angle at different water contents, 7 tests ($T_1$-$T_7$) were performed for unsaturated loess samples of different water contents at four normal stresses (50, 100, 150, 250 kpa) by multistage testing procedure (Stark and Eid, 1994). Another test ($T_8$) was performed for saturated loess sample at normal stress of 250 kpa by single-stage testing procedure (Tiwari and Marui, 2004). Choosing such the two testing procedures is to ensure least variation of the samples and to obtain identical properties related to these samples. The testing procedures will be described in detail in the following section.

To examine whether shear displacement during multistage shearing has impact on shear resistances of soil, 3 ancillary tests ($T_9$-$T_{11}$) were performed by individual shear tests for unsaturated samples with the same water content at a given normal stress under different shear displacements (10, 30, 40 cm). The tests are similar to the single-stage testing for saturated samples. Another 3 ancillary tests ($T_{12}$-$T_{14}$) were conducted by single-stage testing procedure at different normal stresses for saturated samples. These tests aim at achieving void ratio change before and after shearing for a complete analysis.

To perform multistage testing for unsaturated samples, each sample was consolidated at initial normal stress of 50 kpa, and then was sheared at a shear rate of 0.1 mm/s up to steady state at 10 cm shear displacement under drained condition. Then the procedure was repeated on the same sample for the normal stresses of 100, 150 and 250 kpa to obtain cohesion and angle friction of the sample.

To perform single-stage testing for saturated samples, each sample was first saturated with the help of carbon dioxide and de-aired water. The degree of saturation was checked by using the $B_D$ parameter proposed by Sassa (1985), in this study, the samples was fully saturated ($B_D$ = 1.0). The saturated sample was consolidated at normal stress of 250 kpa, and was sheared at shear rate of 0.1 mm/s up to steady state, i.e., until pore pressure and shear resistance remained constant. To obtain the friction angle and cohesion of the saturated sample, the residual failure line (R.F.L.) was measured after the undrained shear test. After the undrained shearing testing was completed, the upper drainage line was switched to a drainage condition so that the generated porewater pressure could dissipate, while the lower part of the ring shear apparatus was kept rotating at a small constant speed (0.1 mm/s). The stress shifted from Point SSP to Point RS1, where the generated pore-water pressure dissipated completely. Thereafter, the loaded normal stress was reduced to a small value at a very slow rate (0.05 kPa/s) after shearing to ensure the drained condition, while the shear resistance was measured. The stress moved from RS1 to RS2. The line between RS1 and RS2 shows the residual failure line (R.F.L.) of this sample. The measured shear resistance can be regarded as the ultimate shear strength for this sample at the applied normal stress (Wang et al., 2007).

To analyze void ratio after consolidation (before shearing) and after shearing, sample height during shearing was recorded concurrently with progress of shear deformation for all of the tests. Additionally, the initial water content was calibrated before each sample was placed into shear box. After shearing was completed, the shear box was opened, and samples were taken from three different layers (i.e., below, within and above the shear zone), and then their water content were measured.

## 3 Results

Because of the imposed sample preparation and testing procedure, the only difference is water content to the unsaturated samples ($T_1$-$T_7$), apart from the tests ($T_9$-$T_{11}$) being used to examine the effect shear displacement on shear resistance. To the saturated samples ($T_8$, $T_{12}$-$T_{14}$), the testing procedure is different from that of unsaturated samples. Hence, we present one example of the unsaturated samples and of the saturated samples, respectively. Furthermore, the results of the tests ($T_9$-$T_{11}$) were presented completely.

### 3.1 Effect of water content on shear strength

To exemplify the shear strength behavior at different water contents, results of unsaturated sample ($T_4$) and saturated sample ($T_8$) are presented in Fig. 4 and 5, respectively.

Fig. 4 shows that the results of multistage shear testing on the unsaturated sample with an initial water content of 12.98% ($T_4$). Fig. 4a shows that variation of shear resistance with progress of shear displacement at four normal stresses. Fig. 4b shows that the variation of sample height with progress of shear displacement. In Fig. 4 it can be seen that the shear resistance maintain a steady state and the sample height decreased gradually with increasing shear displacement.

Fig. 5 shows that the results of single-stage testing on saturated sample ($T_8$). Fig. 5a shows the variation of normal stress, shear resistance, and pore pressure with progress of shear displacement. It is found that some pore pressure was built up before peak shear strength, while after failure, pore pressure showed a sharp increase, and the shear resistance decreased gradually with progress of shear displacement and finally reached a constant, i.e., constant volume, constant normal effective stress and constant velocity (Poulos, 1981). Fig. 5b shows the effective stress path and residual failure line. The measured shear resistance was regarded as the ultimate shear strength for the saturated sample, as suggested by Wang et al. (2007).

Fig.6 summarizes the variation of residual shear strength with normal stress (i.e., failure envelope) on the tests ($T_1$-$T_8$), ranging from 2.97% to 25.03% in water content on shear zone. The slope and the intercept of the failure envelope denoted residual friction angle ($\varphi$) and cohesion ($C$) for each sample, respectively.

3.2 Effect of shear displacement on shear strength

To examine the effect of testing procedure on shear strength behavior, the tree tests ($T_9$-$T_{11}$) were conducted at almost the same initial water content (15.59% ± 0.03) and the same normal stress of 250 kpa. Fig. 7 illustrates the results of variation of stress ratio with different progress of shear displacements (10, 30, 40 cm). As shown in Fig. 7, there is very light increase in stress ratio with progress of shear displacement, but the effect of the increase was negligible to define cohesion and friction angle of sample in our tests. The results show that multistage testing can produce results similar to sing-stage testing, and can obtain identical properties of sample after test. This finding is consistent with those observed in clay tests performed by other authors (Stark and Eid, 1994; Tiwari and Marui, 2004).

3.3 Effect of water content and shearing on void ratio

Fig. 8 shows the variation in void ratio with water content of the samples ($T_1$-$T_8$) at four different normal stresses. Fig. 8a plots void ratio after consolidation (before shearing) against the initial water content before sample was placed into shear box. Fig. 8b plots void ratio after shearing against the water content on shear zone after shearing was finished. The void ratio of each sample was calculated using the variation of sample height after consolidation and shearing (as shown in Fig. 4b) by the formula ($e=G_s/p_d - 1$), in which $G_s$ is specific gravity of the sample, $p_d$ was dry density of the sample at a given normal stress.

In Fig. 8, it can be seen that the void ratio of sample decrease with water content until certain water content threshold, either before or after shearing, and thereafter it begins to increase and reaches a stable state near saturation. It is interesting to note that the threshold is about the plastic limit of the samples. This indicated that the inconsistent change in void ratio is related to the transition of soil state from plastic to liquid.

By comparing Fig.8a to b, it can be found that the void ratio of the samples was higher before shearing (after consolidation) than after shearing until a certain water content threshold (18.47%), the difference decreasing as the samples are close to saturated condition. It shows that the contraction of the samples occurred during shearing.

The comparison also showed that the water content after shearing increased with the reduction of void ratio and is higher than that before test until the water content threshold (18.47%), after which the water content after test decreased with increasing void ratio and is smaller than that of before shearing. This result revealed that the change in water content was accompanied by change in void ratio during shearing.

## 3.4 Shearing-induced change within sample

Change of the samples within shear box, here concerning shear zone and water content, were observed and measured for each test. Fig. 9 shows example of shear zone formed in our tests and a sketch of water content test. Observation of shear deformation of the samples showed that an annular shear zone with a lens-shaped cross section was formed in each test, as shown in Fig. 9a and b. The observation showed that the shear deformation in ring shear tests was localized in the shear zone. This phenomenon is consistent with that observed in sand ring-shear tests performed by Wang and Sassa (2002) and Moore and Iverson (2002).

Fig. 9c presents a sketch of water content test for each test. The samples were taken from layers below, within and above the shear zone, respectively. Because the shear zone is thin (as shown in Fig. 9a and b), we collected totally the shear zone, and divided into three parts. The results showed that the water content within sample changed along shear zone during shearing for all of the tests, causing the development of pore pressure gradient in each sample.

## 4 Discussions

### 4.1 Volumetric response

In our tests the increase of water content resulted in the samples to contraction until the water content threshold (18.47%), whereas the continued increase of water content resulted in the samples to swell compared to the sample before the water content threshold (as shown in Fig. 8). This process was explained because the soil is of metastable structure (Barden et al., 1973; Fredlund and Morgenstern, 1976). Nevertherless, it was well documented that this process has great impact on the changes in physical and mechanical properties of the loess due to volumetric change after wetting (Feda, 1966; Šajgalik, 1990; Derbyshire et al., 1994; Dijkstra, 2001; Kruse et al., 2007). It has also found that the change in water content on shear zone was accompanied by the volumetric change during shearing (Fig. 8). To this kind of phenomenon, Terzaghi et al (1996) have pointed out that it is related to change in density of soil during shearing, and this can modify shear resistance. Clearly, volumetric response of soil during wetting and shearing is of great importance to understand variations of shear strength parameters and water migration in our tests.

## 4.2 Cohesion and friction angle

The effect of water content on cohesion (*C*) and friction angle ($\varphi$) is illustrated in Fig. 10, where *C* and $\varphi$ are plotted against the water content on shear zone for the tests ($T_1$-$T_8$). As shown, with an increase in water content, *C* increased and $\varphi$ decreased until the water content threshold (18.47%), and thereafter, *C* decreased quickly to zero and $\varphi$ increased lightly and then stabilized at a residual value. This phenomenon is similar to that obtained in ring shear tests on the Lanzhou loess performed by Derbyshire et al. (1994) and Dijkstra et al. (1994). They explained that this phenomenon is related to the bonds between particles influenced by thickness change of water molecules surrounding particles when the water content increases. However, the nature of bands between particles is extremely complex (Barden et al., 1973; Terzaghi et al., 1996; Craig, 2004). Here, this phenomenon shown in Fig. 10 was explained in terms of the volumetric change during wetting as follows.

The friction angle should represent only the contribution of physical bonding to shear resistance for uncemented soil (Terzaghi et al., 1996). This means that the friction angle of uncemented soil is only dependent on the shear resistance of soil, which in turn depends on effective normal stress (Terzaghi et al., 1996; Craig, 2004). Therefore, the friction angel of uncemented soil should be a function of shear resistance or effective normal stress. In our tests the samples are not related to cementation because the tests were conducted on completely remolded samples (Derbyshire et al., 1994; Dijkstra et al., 1994). It is has well known that the increase of water content and the reduction of void ratio will result in the increase of the pore water pressure, causing the reduction of effective normal stress (Barden et al., 1973; Terzaghi et al., 1996; Craig, 2004). Therefore, in our tests the friction angle decreased gradually with decreasing effective normal stress when the water content is continuously close to the threshold (18.47%), after which the friction angel retained a stable value as the sample reached constant, i.e. constant volume and constant effective normal stress. The process is consistent with change in residual shear resistance with increasing water content, as shown in Fig. 11.

The cohesion of soil is attributed to negative pore water pressure within void space very small in size between particles (Craig, 2004). The negative pore water pressure is also referred to as soil suction that mainly depends on pore size and water content (Fredlurid and Rahurcjo, 1993; Vanapalli et al., 1996; Craig, 2004). It was well documented that the suction will increase with decreasing void ratio and water content (Fredlurid and Rahurcjo, 1993; Craig, 2004). In our tests, this appears to have a paradox that the change in suction with the increase of water content and the reduction of void ratio. However, the previous research has shown that the suction of silt with metastable structure increase with decreasing void ratio, even though the water content was always an increasing variable before a critical value (Matyas and Radhakrishna, 1968; Fredlund and Morgenstern, 1976). Furthermore, it was well documented that the Lanzhou loess is typically metastable structure silt (Derbyshire et al., 1994; Dijkstra et al., 1994; Derbyshire, 2001; Dijkstra, 2001; Kruse et al., 2007).

Therefore, we concluded that the change in cohesion of the samples is related to suction of soil, although the suction was not measured in our tests. Before the water content threshold (18.47%), the cohesion increased due to the increase of suction, because a reduction in void ratio resulted in a reduction in pore size between particles, causing the increase of suction. After the water content threshold (18.47%), metastable structure of soil was destroyed when the water content increase continuously, and then an increase in void ratio caused an increase in pore size between particles, leading to the very limited suction and high pore-water pressure, and as a result, the cohesion deceased rapidly to zero.

4.3 Water migration

The water content change within samples for the tests ($T_1$-$T_8$) was illustrated Fig. 12 for a better comparison, although the phenomenon of water migration occurred in all of the tests. In Fig. 12, we found two different types of water migration on shear zone. The first one is that water migrate towards the shear zone from the soil layers below and above the shear zone, as the water content is smaller than 18.47%, and thereafter, the second one occurs, is that water migrate outwards the shear zone into the soil layers below and above the shear zone. The comparison of void ratio and water content before and after shearing (as shown in Fig. 8) has shown that the water migration, which is related to volumetric change during shearing, depends on the pre-shear water content.

In our tests, the volumetric change during shearing may be localized on the shear zone, or is at least very much stronger on shear zone than on soil layers above and below the shear zone, because the shear deformation was localized on the shear zone in ring shear tests (Fig. 9a and b). In other words, there is a distinct difference between shear zone and others position within samples due to the localization of shear deformation. The kind of difference has been observed from special attention to shear zone in ring shear tests (Wang and Sassa, 2002; Wafid Agung et al., 2004; Fukuoka et al., 2006; Wang and Sassa, 2009). The following explanation to water migration will be focus on the difference.

To the first type, the void ratio of shear zone is lower than that of the soil layers above and below the shear zone due to localization of shear deformation. As a result the suction is higher on shear zone than on soil layers above and below the shear zone, because the suction increase with decreasing void ratio at a given condition (Fredlurid and Rahurcjo, 1993). Therefore, the water migrated towards the shear zone during shearing as a result of pore-volume change along shear zone.

To the second type, the suction of soil is very limited due to high saturation (Fredlurid and Rahurcjo, 1993; Vanapalli et al., 1999), although the void ratio is still lower on shear zone than in the soil layers above and below the shear zone. However, Terzaghi et al. (1996) have suggested that in saturated soils density change during shearing is achieved by expelling or by taking in water. Therefore, the reduction of water content on shear zone is related to the reduction of void ratio along shear zone. The results in our tests showed that this kind of phenomena also occur near to saturated soils.

It has been reported that the evident reduction of shear strength on overconsolidated clay samples was attributed to the light increase of water content on shear zone in undrained triaxial tests (Bishop, 1961; Skempton and La Rochelle, 1965), whereas other studies have shown that the reduction of water content on shear zone can increase the shear strength on saturated sensitive clay samples in undrained triaxial tests (Taylor, 1951; Crawford, 1961). The above results, along with our test results showed that the water migration on shear zone is different for different types of soil, even though the sample were all located in saturated condition. However, it is clear that the water migration has great impact on shear strength of soil, and that the effect is dependent on the type of water migration on shear zone. Furthermore, the magnitude of the effect of water migration on shear strength may have difference to different soils. The effect of water migration on shear strength can be concluded as follows, although in our tests concurrent changes in water migration and mobilized shear strength could not be measured. If the water migrate towards shear zone, shear strength on shear zone may be decease due to the reduction of suction or the increase of pore pressure. If the water migrate outwards shear zone, the shear strength may be increase due to the reduction of water content on shear zone.

## 5 Conclusions

A series of tests were conducted on loess to examine their shear behavior of using a ring shear apparatus. Based on test results presented in this paper, the following conclusions can be drawn.

(1) The increase of water content caused the reduction of void ratio of the samples until the water content threshold of 18.47%, and thereafter, the continued increase of water content caused the light increase of void ratio then reached a stable state. Furthermore, contraction during shearing occurred in all of the tests due to the reduction of void ratio.

(2) The cohesion increased and the friction angle decreased with increasing water content until the water content threshold of 18.47%, after which the cohesion decreased quickly to zero and the friction angle increased lightly and then stabilized at a residual value.

(3) The localization of shear zone was accompanied by shear deformation for all of the tests. The two types of water migration on shear zone occurred in our

tests. The water was sucked towards shear zone from soil layers above and below the shear zone when the water content is smaller than 18.47%, whereas thereafter the water was expelled shear zone into soil layers above and below the shear zone.

(4) The effect of water migration on shear strength of soil depends on the type of water migration on shear zone. The water migration may play a negative role in decreasing shear strength when water migrate towards shear zone, whereas it may play a positive role in increasing shear strength when water migrate outwards shear zone.

(5) There was a same water content threshold for changes in void ratio, strength parameters and water migration. The threshold is close to the plastic limit of the samples. All of the changes revealed the dependence of the shear behavior and the water migration on soil volumetric response during wetting and shearing.

**Acknowledgements**

This study was supported by the National Natural Science Foundation of China (Nos. 41977212 and 42090053), and National Key Research and Development Program of China (2022YFC3003401).

## Reference:


Abduljauwad, S.N., Al-Gassous, K.A., 1991. Soil deformation and shear strength characteristics of the Sana'a soil, Yemen Arab Republic. Engineering Geology 31, 291-314.

Audric, T., Bouquier, L., 1976. Collapsing behaviour of some loess soils from Normandy. Quarterly Journal of Engineering Geology and Hydrogeology 9, 265-277.

Barden, L., McGown, A., Collins, K., 1973. The collapse mechanism in partly saturated soil. Engineering Geology 7, 49-60.

Bishop, A.W., 1961. Discussion on soil properties and their measurement. Proc. 5th Int. Conf. Soil Mech., Paris, pp. 89-93.

Bishop, A.W., Green, G.E., Garga, V.K., Andresen, A., Brown, J.D., 1971. A new ring shear apparatus and its application to the measurement of residual strength. Géotechnique 21, 273-328.

Bromhead, E.N., 1979. A simple ring shear apparatus. Ground Engineering 12, 40-44.

Craig, R.F., 2004. Craig's Soil Mechanics, 7th Edition. Taylor & Francis Group.

Crawford, C.B., 1961. The influence of strain on shearing resistance of sensitive clay. ASTM 61, 1250-1265.

Derbyshire, E., 2001. Geological hazards in loess terrain, with particular reference to the loess regions of China. Earth-Science Reviews 54, 231-260.

Derbyshire, E., Dijkstra, T.A., Smalley, I.J., Li, Y., 1994. Failure mechanisms in loess and the effects of moisture content changes on remoulded strength. Quaternary International 24, 5-15.

Derbyshire, E., Wang, J., Jin, Z., Billard, A., Egels, Y., Kasser, M., Jones, D.K.C., Muxart, T., Owen, L., 1991. Landslides in the Gansu loess of China. Catena Supplement 20, 119-145.

Dijkstra, T.A., 2001. Geotechnical thresholds in the Lanzhou loess of China. Quaternary International 76-77, 21-28.

Dijkstra, T.A., Rogers, C.D.F., Smalley, I.J., Derbyshire, E., Li, Y.J., Meng, X.M., 1994. The loess of north-central China: Geotechnical properties and their relation to slope stability. Engineering Geology 36, 153-171.

Feda, J., 1966. Structural stability of subsident loess soil from Praha-Dejvice. Engineering Geology 1, 201-219.

Finno, R.J., Harris, W.W., Mooney, M.A., Viggiani, G., 1997. Shear bands in plane strain compression of loose sand. Geotechnique 47, 149-165.

Fredlund, D.G., Morgenstern, N.R., 1976. Constitutive relations for volume change in unsaturated soils. Canadian Geotechnical Journal 13, 261–276.

Fredlurid, D.G., Rahurcjo, H., 1993. Soil Mechanics for Unsaturated Soils. John Wiley & Sons, Inc.

Fukuoka, H., Sassa, K., Wang, G., Sasaki, R., 2006. Observation of shear zone development in ring-shear apparatus with a transparent shear box. Landslides 3, 239-251.

Gibbs, H.J., Holland, W.Y., 1960. Petrographic and engineering properties of loess. U.S. Bureau of Reclamation, Denver. Engineering Monographs 28, 1-37.

Ishihara, K., Okusa, S., Oyagi, N., Ischuk, A., 1990. Liquefaction- induced flowslide in the collapsible loess deposit in Soviet Tajik. Soils and Foundations 30, 73-89.

Kruse, G.A.M., Dijkstra, T.A., Schokking, F., 2007. Effects of soil structure on soil behaviour: Illustrated with loess, glacially loaded clay and simulated flaser bedding examples. Engineering Geology 91, 34-45.

Long, J., Li, T., Lei, X., Yang, S., 2007. Study on physical properties of soil in sliding zone of loess landslide. Chinese Journal of Geotechnical Engineering 29, 289-293. (in Chinese).

Lutenegger, A.J., 1981. Stability of loess in light of the inactive particle theory. Nature 291, 360-360.

Lutenegger, A.J., Hallberg, G.R., 1988. Stability of loess. Engineering Geology 25, 247-261.

Matyas, E.L., Radhakrishna, H.S., 1968. Volume change characteristics of partially saturated soil. Géotechnique 18, 432-448.

Moore, P.L., Iverson, N.R., 2002. Slow episodic shear of granular materials regulated by dilatant strengthening. Geology 30, 843-846.

Phien-wej, N., Pientong, T., Balasubramaniam, A.S., 1992. Collapse and strength characteristics of loess in Thailand. Engineering Geology 32, 59-72.

Poulos, S.J., 1981. The steady state of deformation. Journal of the Geotechnical Engineering Division, ASCE 107, 553-562.

RenéJacques, B., 1988. Some specific problems of wetted loessial soils in civil engineering. Engineering Geology 25, 303-324.

Šajgalik, J., 1990. Sagging of loesses and its problems. Quaternary International 7-8, 63-70.

Sassa, K., 1985. The mechanism of debris flows. In Proceedings of the 11th International Conference on Soil Mechanics and Foundation Engineering, San Francisco, Calif. Vol. 3, pp. 1173–1176.

Sassa, K., Fukuoka, H., Wang, G., Ishikawa, N., 2004. Undrained dynamic-loading ring-shear apparatus and its application to landslide dynamics. Landslides 1, 7-19.

Sassa, K., Wang, G., Fukuoka, H., 2003. Performing undrained shear tests on saturated sands in a new intelligent type of ring shear apparatus. Geotechnical Testing Journal 26, 257-265.

Skempton, A.W., La Rochelle, P., 1965. The Bradwell slip: A short-term failure in London Clay. Géotechnique 15, 221-242.

Stark, T.D., Eid, H.T., 1994. Drained Residual Strength of Cohesive Soils. Journal of geotechnical engineering 120, 856-871.

Tan, T.K., 1988. Fundamental properties of loess from Northwestern China. Engineering Geology 25, 103-122.

Taylor, D.W., 1951. Research on shearing resistance of clay: Sections on water migration studies. U.S. Army Engineers Waterways Experiment Station Report 36-42, 9-12.

Terzaghi, K., Peck, R.B., Mesri, G., 1996. Soil Mechanics in Engineering Practice, 3rd Edition. John Wiley & Sons, Inc.

Tiwari, B., Marui, H., 2004. Objective Oriented Multistage Ring Shear Test for Shear Strength of Landslide Soil. Journal of Geotechnical and Geoenvironmental Engineering 130, 217-222.

Ueno, M., Nishimura, T., Kato, M., Nakamura, H., Zeng, S., 2005. Variation of shearing characteristics of loess soil after irrigation. Northwestern Seismological Journal 27, 128-134.

Vanapalli, S.K., Fredlund, D.G., Pufahl, D.E., 1996. The Relationship Between the Soil-Water Characteristic Curve and the Unsaturated Shear Strength of a Compacted Glacial Till. Geotechnical Testing Journal 19, 259-268.

Vanapalli, S.K., Fredlund, D.G., Pufahl, D.E., 1999. The influence of soil structure and stress history on the soil-water characteristics of a compacted till. Géotechnique 49, 143-159.

Wafid Agung, M., Sassa, K., Fukuoka, H., Wang, G., 2004. Evolution of Shear-Zone Structure in Undrained Ring-Shear Tests. Landslides 1, 101-112.

Wang, G., Sassa, K., 2002. Post-failure mobility of saturated sands in undrained load-controlled ring shear tests. Canadian Geotechnical Journal 39, 821-837.

Wang, G., Sassa, K., 2009. Seismic loading impacts on excess pore-water pressure maintain landslide triggered flowslides. Earth Surface Processes and Landforms 34, 232-241.

Wang, G., Sassa, K., Fukuoka, H., Tada, T., 2007. Experimental Study on the Shearing Behavior of Saturated Silty Soils Based on Ring-Shear Tests. Journal of Geotechnical and Geoenvironmental Engineering 133, 319-333.

Wang, G., Suemine, A., Schulz, W.H., 2010. Shear-rate-dependent strength control on the dynamics of rainfall-triggered landslides, Tokushima Prefecture, Japan. Earth Surface Processes and Landforms 35, 407-416.

Zhang, D., Wang, G., 2007. Study of the 1920 Haiyuan earthquake-induced landslides in loess (China). Engineering Geology 94, 76-88.

Zhang, D., Wang, G., Luo, C., Chen, J., Zhou, Y., 2009. A rapid loess flowslide triggered by irrigation in China. Landslides 6, 55-60.

**Table captions:**

Table 1. Basic physical properties of loess used in this study

**Figure captions:**

Fig.1 Location of study area and sampling site

Fig. 2 Grain size distributions curve of loess used in this study

Fig. 3 Ring-shear apparatus DPRI-Ver.5. (a) Overview of the ring shear apparatus with a transparent shear box; (b) Sample in ring-shear apparatus; (c) Cross section through center of undrained shear box of ring-shear apparatus.

Fig. 4 Example of Drained shear test on the unsaturated sample. (a) Shear resistance against shear displacement at different normal stresses. (b) Sample height against shear displacement at different normal stresses.

Fig. 5 Undrained shear test on the saturated sample ($T_8$). (a) Variation of normal stress, pore pressure, and shear resistance with shear displacement. (b) Residual failure line and effective stress path.

Fig. 6 Residual shear strength against normal stress at different water contents one shear zone for the test ($T_1$-$T_8$).

Fig. 7 Stress ratio against shear displacement on samples with the same water content at a given normal stress.

Fig. 8 Void ratio against water content at different normal stresses. (a) Void ration against initial water content after consolidation (before shearing). (b) Void ration against final water content on shear zone after shearing at each shear steps.

Fig. 9 Example of shear zones on the sample T4. (a) Formation of the shear zone after shearing; (b) Change in basic properties of the shear zone (c) Sketch map of water content test at different soil layers.

Fig. 10 Cohesion and residual friction angle at different water contents.

Fig. 11 Shear resistance against water content at different normal stresses.

Fig. 12 Water content of samples at different soil layers.

Table 1. Basic physical properties of loess used in this study

| Property (definition and method) | Loess |
|---|---|
| Specific gravity ($G_s$) | 2.71 |
| Initial moist bulk density ($g/cm^3$) | 1.50 |
| Initial water content (%) | 7.40 |
| Initial void ratio | 0.92 |
| Liquid limit (%) | 27.74 |
| Plastic limit (%) | 17.68 |
| Plasticity index (%) | 10.06 |

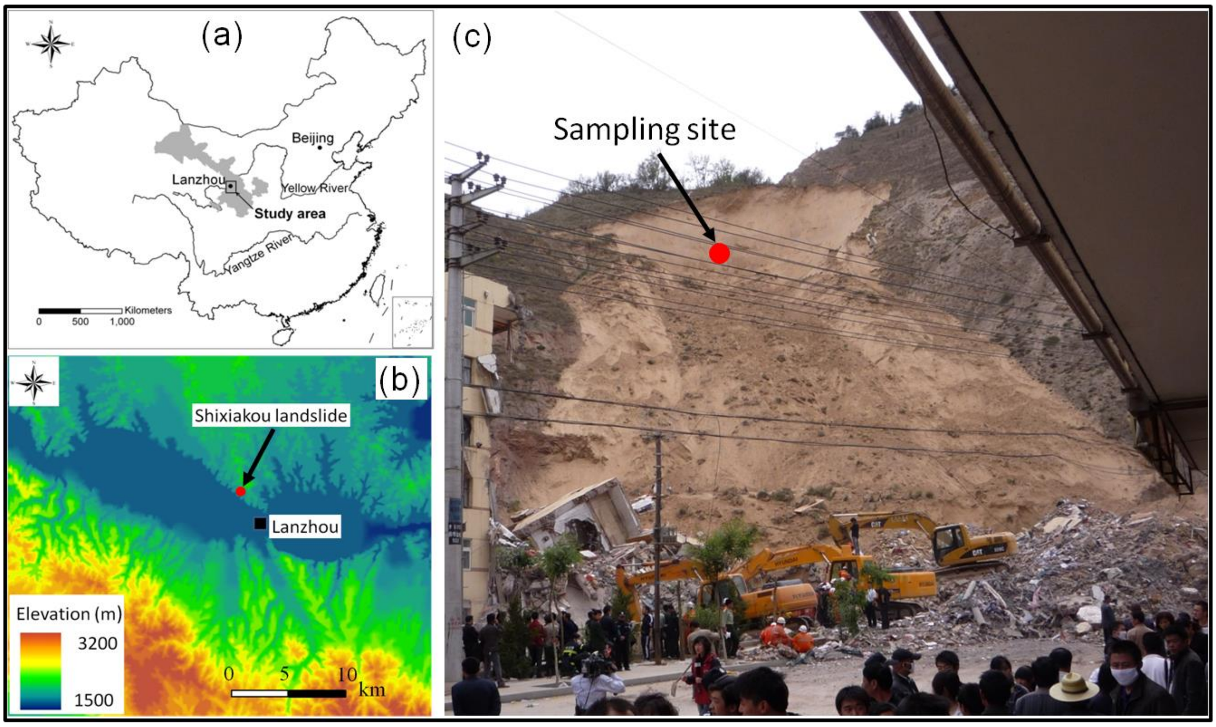


Fig.1 Location of study area and sampling site.

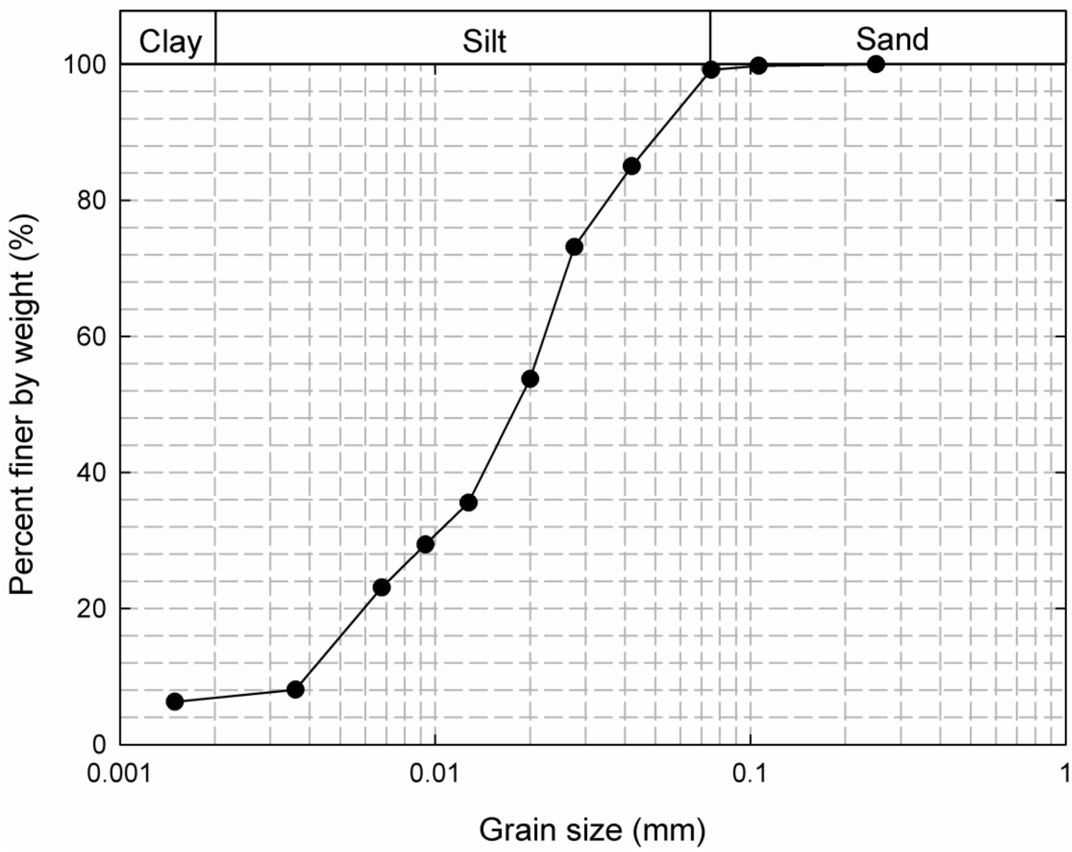


Fig. 2 Grain size distributions curve of loess used in this study.

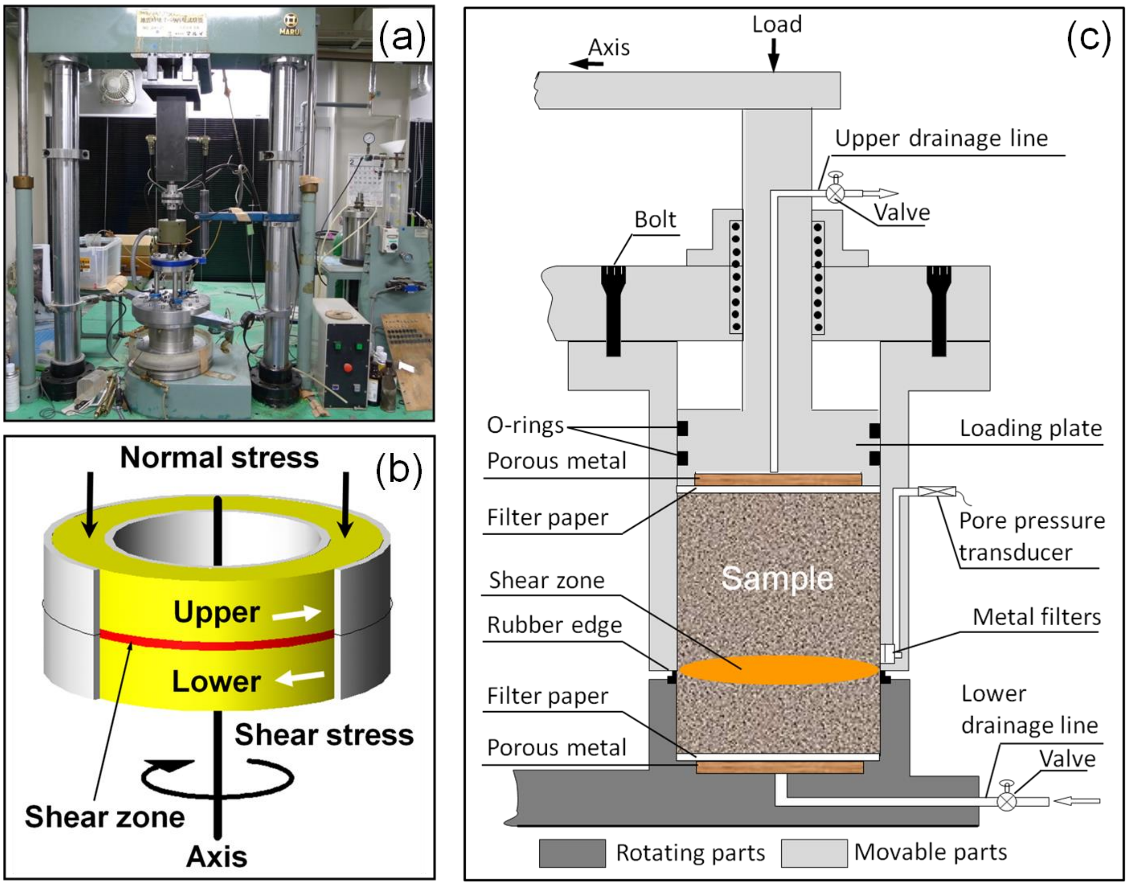


Fig. 3 Ring-shear apparatus DPRI-Ver.5. (a) Overview of the ring shear apparatus with a transparent shear box; (b) Sample in ring-shear apparatus; (c) Cross section through center of undrained shear box of ring-shear apparatus.

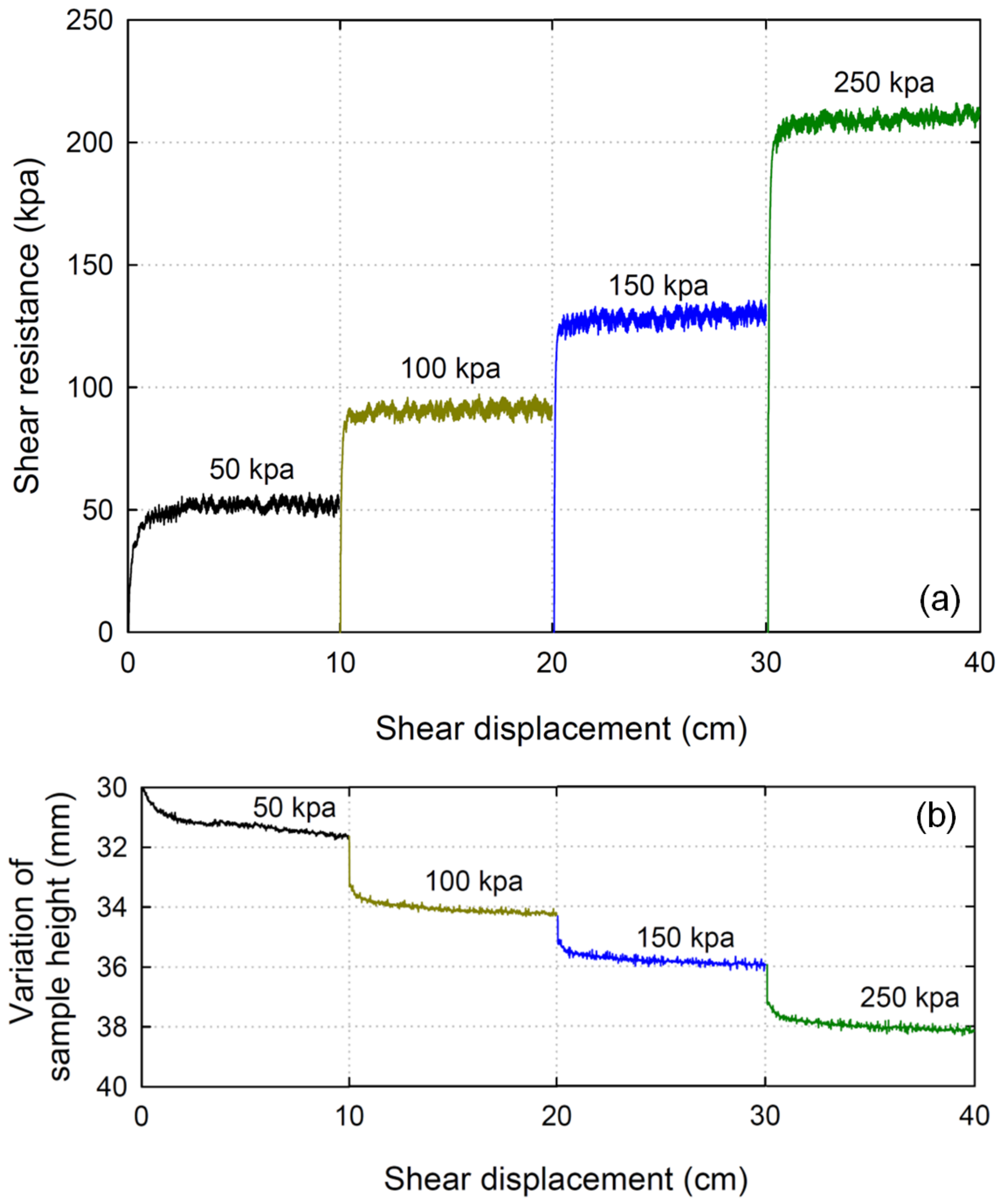


Fig. 4 Example of Drained shear test on the unsaturated sample. (a) Shear resistance against shear displacement at different normal stresses. (b) Sample height against shear displacement at different normal stresses.

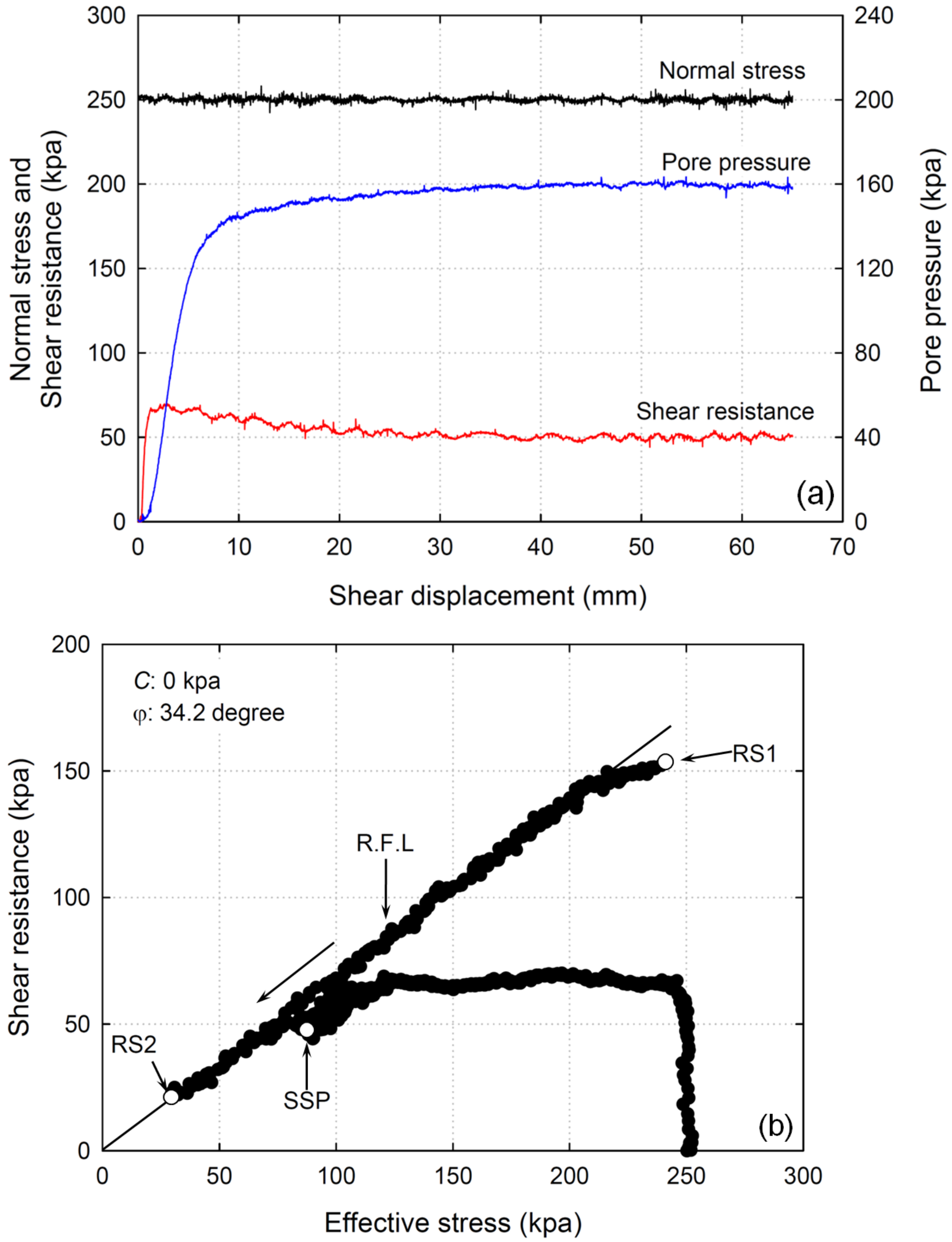


Fig. 5 Undrained shear test on the saturated sample ($T_8$). (a) Variation of normal stress, pore pressure, and shear resistance with shear displacement. (b) Residual failure line and effective stress path.

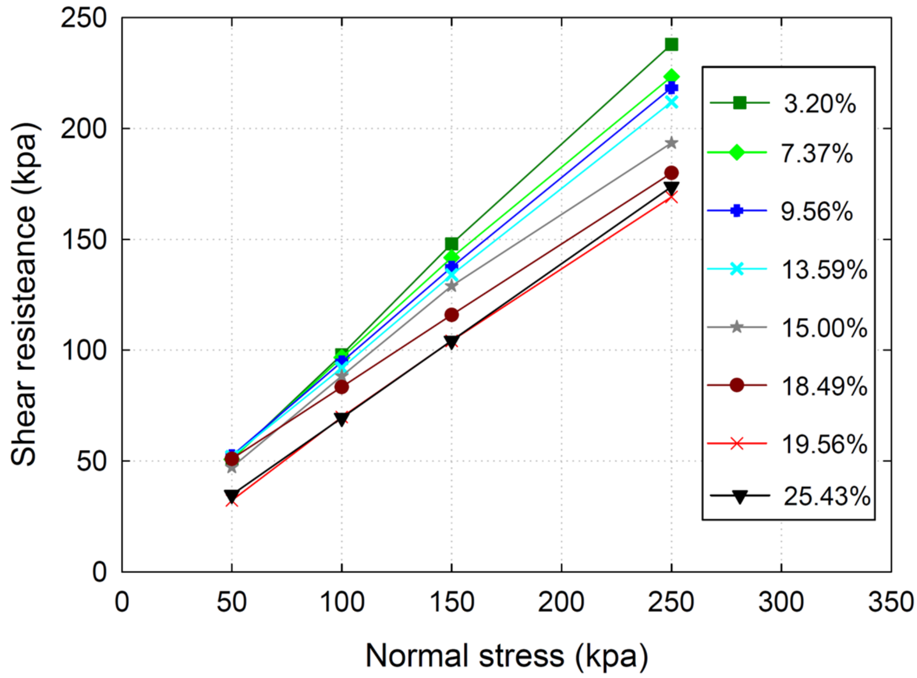


Fig. 6 Residual shear strength against normal stress at different water contents one shear zone for the tests ($T_1$-$T_8$).

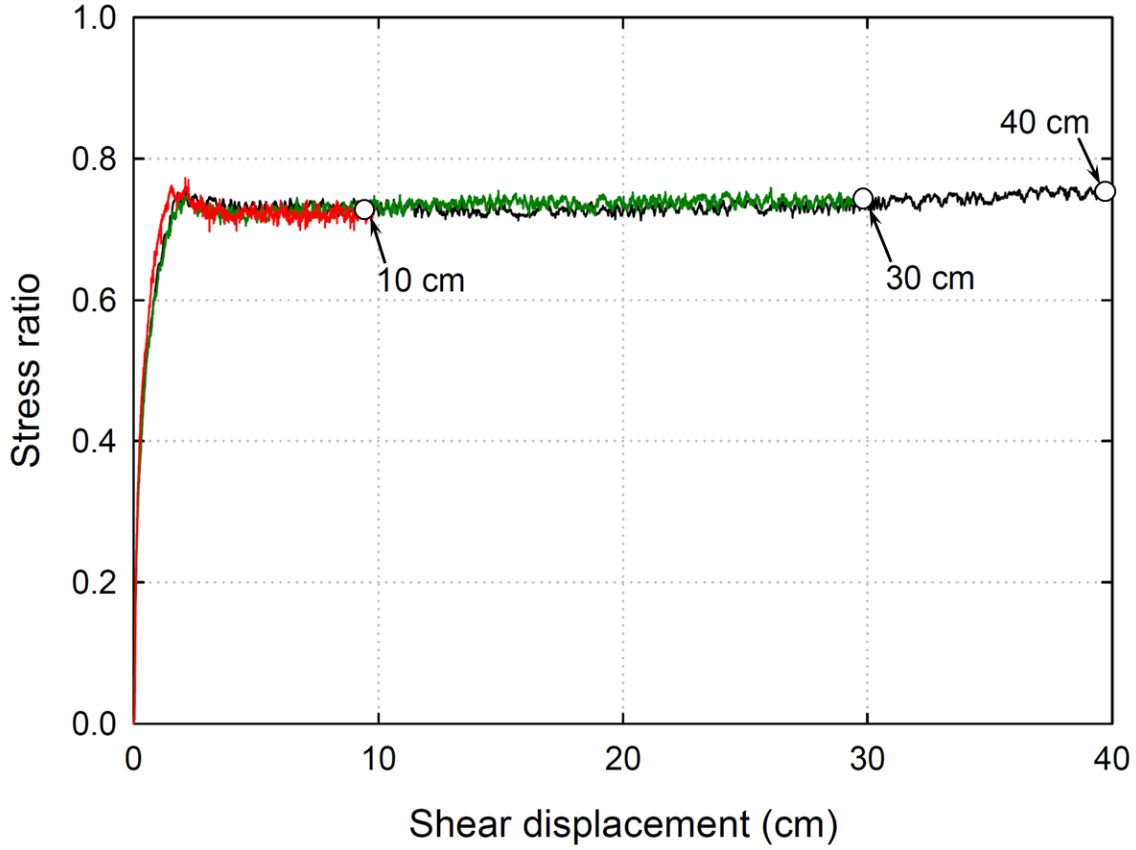


Fig. 7 Stress ratio against shear displacement on samples with the same water content at a given normal stress.

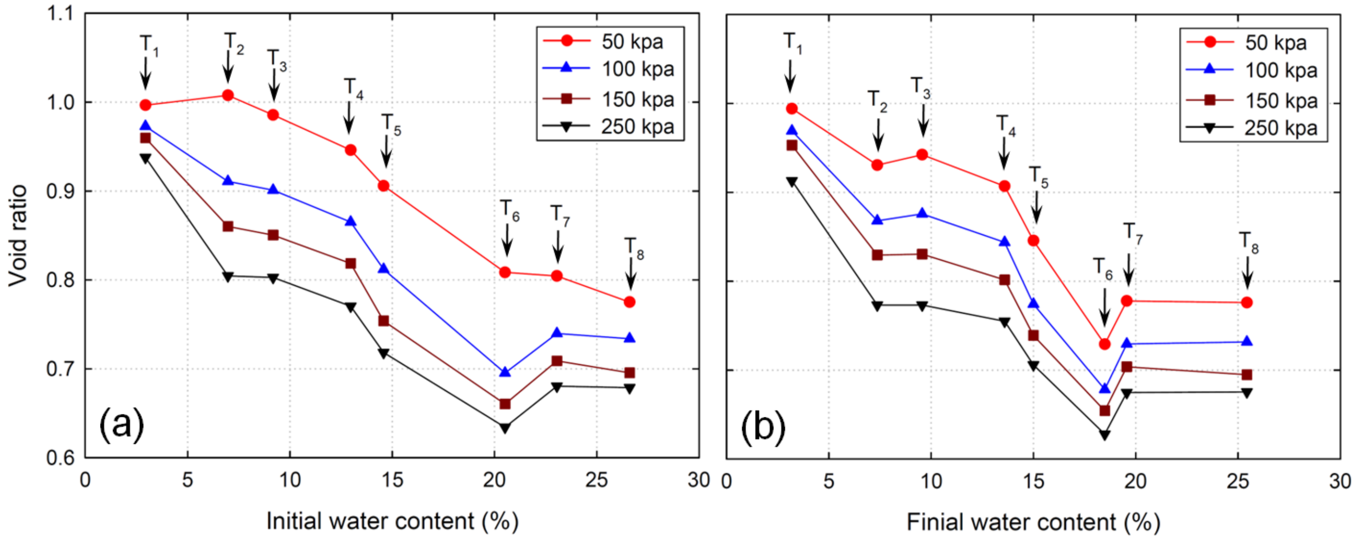


Fig. 8 Void ratio against water content at different normal stresses. (a) Void ration against initial water content after consolidation (before shearing). (b) Void ration against final water content on shear zone after shearing at each shear steps.


(a)
Shear zone

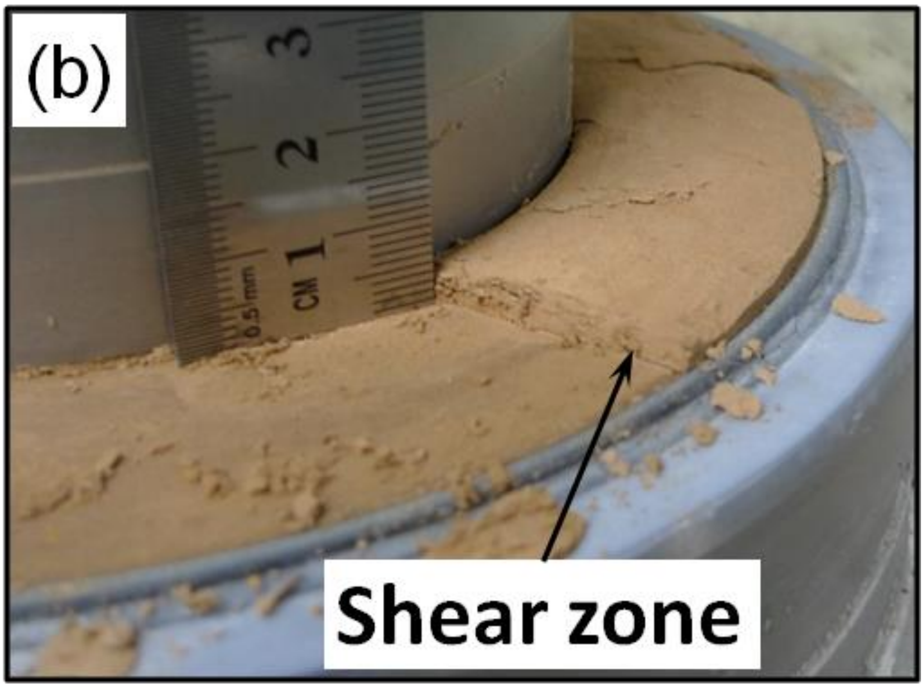
(b)
Shear zone

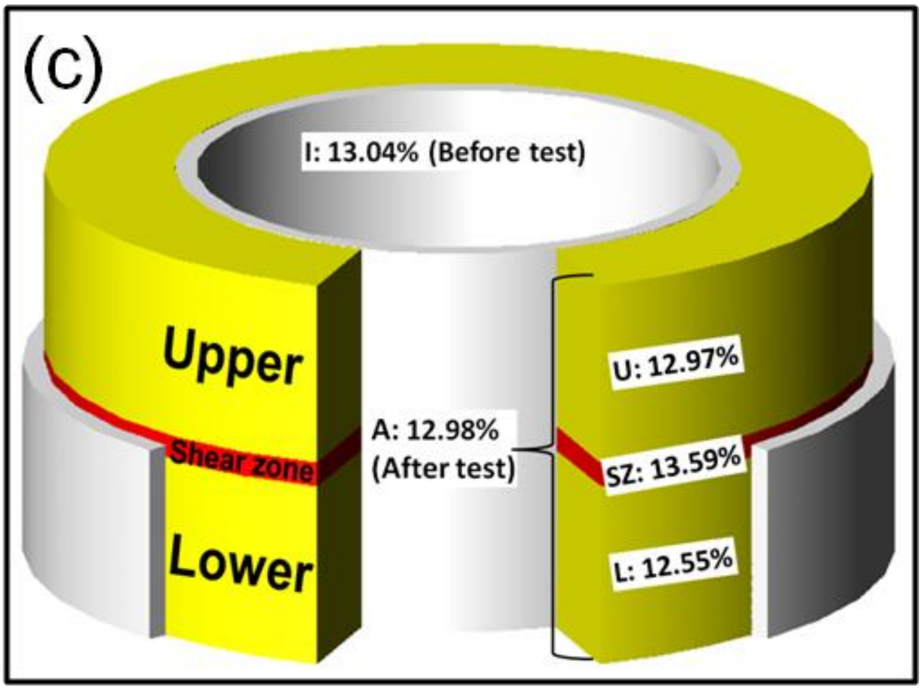


Fig. 9 Example of shear zones on the sample $T_4$. (a) Formation of the shear zone after shearing; (b) Change in basic properties of the shear zone (c) Sketch map of water content test at different soil layers.

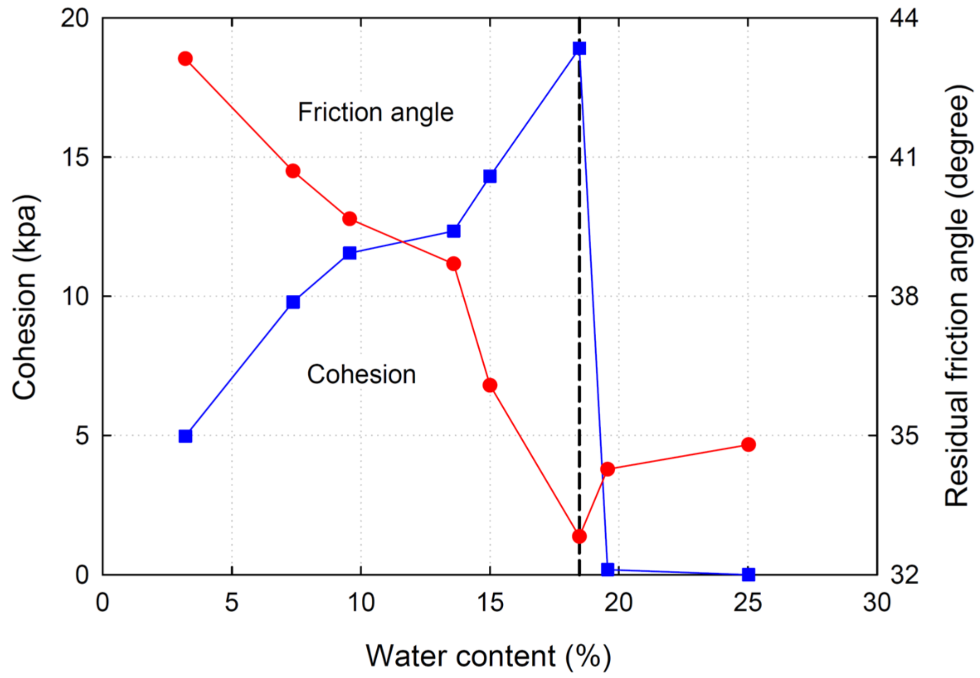


Fig. 10 Cohesion and residual friction angle at different water contents.

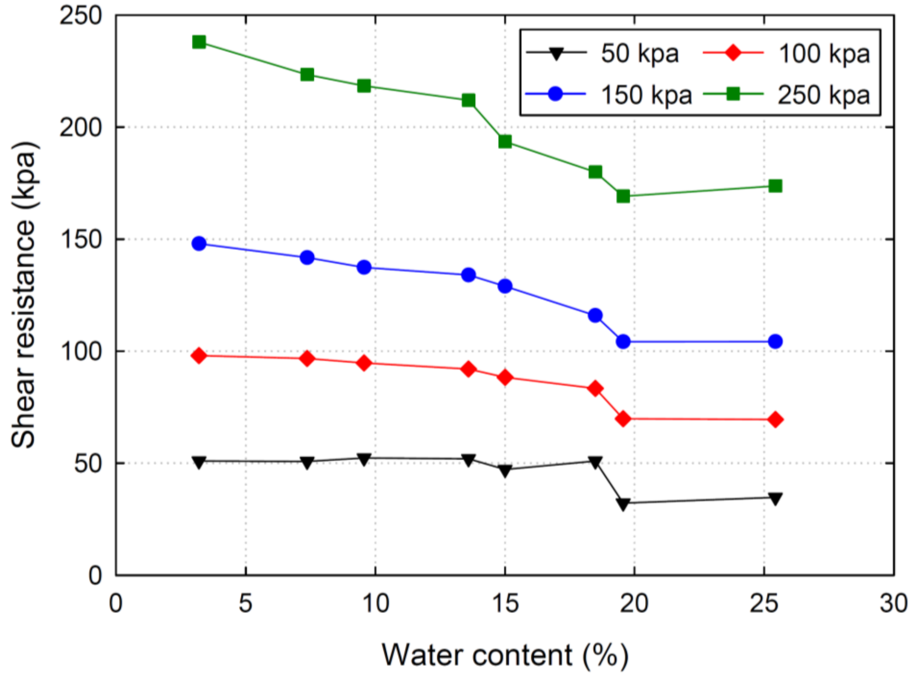


Fig. 11 Shear resistance against water content at different normal stresses.

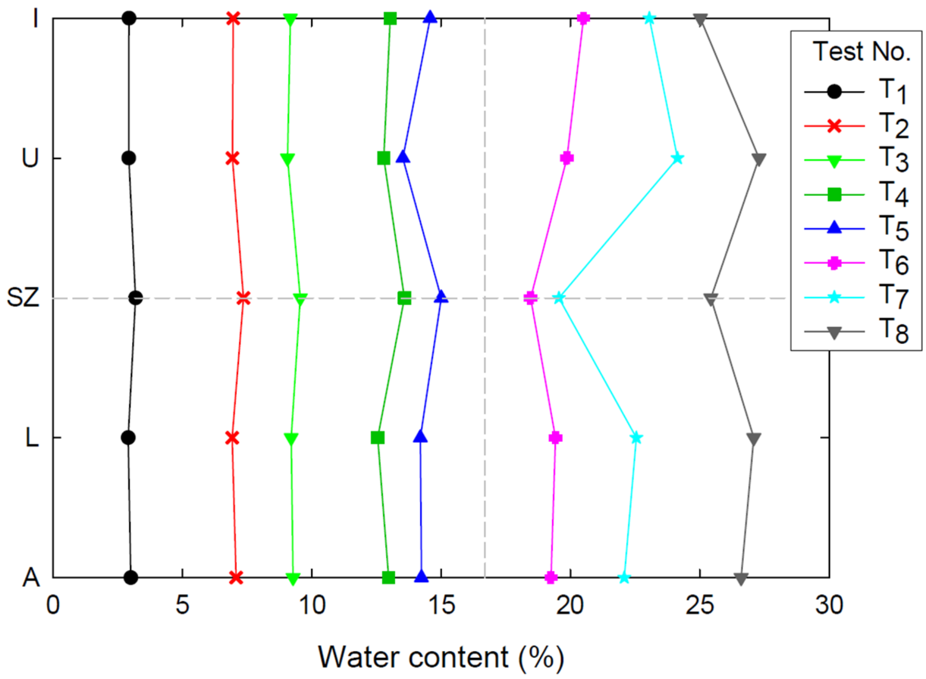


Fig. 12 Water content of samples at different soil layers.

**Note:** I: initial water content before test; U, L: water content of soil layer above and below the shear zone; SZ: water content of soil layer on the shear zone; A: average water content of sample after test